Cement and Concrete Research 123 (2019) 105800

Contents lists available at ScienceDirect

Cement and Concrete Research

journal homepage: www.elsevier.com/locate/cemconres

Ettringite-based binder from ladle slag and gypsum – The effect of citric acid on fresh and hardened state properties

Hoang Nguyen[a], Paivo Kinnunen[a], Katrijn Gijbels[b], Valter Carvelli[c], Harisankar Sreenivasan[a], Anu M. Kantola[d], Ville-Veikko Telkki[d], Wouter Schroeyers[b], Mirja Illikainen[a,*]

[a] Fibre and Particle Engineering Research Unit, University of Oulu, Pentti Kaiteran katu 1, 90014 Oulu, Finland
[b] Nuclear Technological Centre, Hasselt University, Agoralaan, Gebouw H, 3590 Diepenbeek, Belgium
[c] Department A.B.C., Politecnico di Milano, Piazza Leonardo Da Vinci 32, 20133 Milan, Italy
[d] NMR Research Unit, University of Oulu, Pentti Kaiteran katu 1, 90014 Oulu, Finland

ARTICLE INFO

Keywords:
Retardation (A)
Hydration products (B)
Ettringite (D)
Monosulfate (D)
Sulfoaluminate (D)

ABSTRACT

The retardant effects of citric acid on the properties of ettringite binders are not yet fully understood. This investigation provides insights into the effects of citric acid on both the fresh and hardened state properties of the binder produced from the hydration between ladle slag and gypsum (LSG). The results revealed that LSG's initial setting time could be controlled via different citric acid contents and could range from 20 min to 2 h. Citric acid is effective at relatively high dosages; in its absence, ettringite formed almost immediately directly following exposure to water. The presence of citric acid alters the hydration reactions in LSG. AFm was found to be one of main hydration products; citric acid promoted the conversion from ettringite to monosulfate, detected by using solid-state ^{27}Al magic-angle spinning nuclear magnetic resonance spectroscopy. In addition, citric acid increased the compressive strength of LSG mortars by up to 45%.

1. Introduction

Ladle slag (LS) has been successfully used to produce an ettringite-based binder. The steelmaking by-product can form ettringite ($C_3A\bullet3C\overline{S}\bullet32H$) via hydration between Al-rich phases (e.g., mayenite $C_{12}A_7$) and a source of sulfur and calcium: gypsum (G) [1,2]. In addition, the ettringite-based binders exhibit advantages compared to ordinary Portland cement (OPC) due to their high early-age strength [2,3], good chemical resistance [4], and their ability to stabilize heavy metals within their structure [5]. Previous study [2] has already examined the mechanical properties, durability, and phase characterization of the ettringite-based binder (i.e., LSG). Moreover, LSG has been used to develop a strain-hardening cementitious composite with comparable mechanical properties to conventional high-performance OPC-based composites with very low CO_2 emissions [6]. Therefore, the binder can potentially partially replace OPC in order to achieve environmental and economic benefits while attaining high mechanical performance.

The hydration process in ettringite-based binders usually happens quickly. As reported in the literature [7–9], ettringite-based binders' rapid setting (i.e., initial setting time of roughly 10 min) is due to the associated increased rate of hydration reaction [9]. In super sulfated slag cement, the hydration kinetics mainly depends on alkali activator and calcium sulfate content [10]. As for LS, $C_{12}A_7$ is a highly reactive phase, leading to very fast hydration to form ettringite [3,9]. As reported in [3], the mortar composed of LS and dehydrated gypsum hardened in < 4 min if no retarder was used. In contrast, with the addition of a 0.5 wt% retarder, the same mortar can attain the longest initial setting time of 2 h, which is an appropriate setting time for cementitious materials. In addition, the mixture obtained very good compressive strength (approximately 45 MPa after 28 days). It is worth mentioning that a binder's setting time can be considered as the initiation of solidification and subsequent hardening (i.e., the compressive strength gain) [7]. Therefore, prolonging ettringite-based binders' setting time plays an important role in the material's workability and mechanical strength development.

Citric acid can be used to retard the ettringite-forming reaction between Al-rich phases and gypsum. As reported in [3], citric acid added at 0.5 wt% to the mortar prolonged the initial setting time along with the presence of gypsum. In addition, in [2], the concentration of citric acid solution was 0.8 wt% in order to obtain an initial setting time of around 1 h. In the literature, the acid was also proven to be an effective retarder in ettringite-based binders [11–13]. The retarder affected the formation of ettringite crystals during the hydration between

* Corresponding author.
E-mail address: mirja.illikainen@oulu.fi (M. Illikainen).

https://doi.org/10.1016/j.cemconres.2019.105800
Received 11 January 2019; Received in revised form 18 June 2019; Accepted 24 June 2019

calcium aluminate and calcium sulfate sources [12]. Furthermore, the acid has been employed as an additive to improve the setting time and workability of gypsum plasters [14,15]. The proposed mechanism, as in [16], is to prevent nucleation, and hence, ettringite's crystal forming process. However, the effects of citric acid content on both the fresh and hardened states of by-product-based ettringite binders and hydration products are still unclear [2,3,11]. Moreover, only a limited amount of published data deal with the effects of citric acid on the workability and hydration kinetics of ettringite-based binders (see e.g., [13]).

This experimental study aims to provide insights into the effects of citric acid as a retarder on both the fresh and hardened states of LSG. The former was investigated by observing the setting time, heat of hydration (measured by isothermal calorimetry), and in situ XRD. The latter was characterized by ex situ XRD, solid-state ^{27}Al MAS NMR spectroscopy, and compressive strength. The mass concentrations of citric acid used here were 0.1%, 0.5%, 1%, and 2%. LSG without citric acid was considered as the plain reference mixture for comparison. Evaluating LSG in both states provides a better understanding of the effects of citric acid on LSG mixture and its hydration kinetics as well as its effect on other ettringite-based binders in the literature when using the acid as a retarder.

2. Materials and experimental methods

2.1. Materials

SSAB Europe Oy (Finland) provided the LS; the slag was collected from a cooling pit at Raahe (Finland) and exposed to natural weathering. The LS was then sieved using a 2 mm sieve to remove all the leftover steel flakes before being milled with a ball mill (TPR-D-950-V-FU-EH by Germatec, Germany) to reach a d_{50} value of approximately 10 μm, as suggested in [17] and similar to that of OPC. The free CaO in the LS was zero.

VWR Finland supplied the commercial synthetic gypsum (product code 22451.360), which previous investigations have also used [2,18]. The chemical compositions of the LS and gypsum were analyzed with X-ray fluorescence (XRF) (PANalytical Omnian Axiosmax) at 4 kV (see Table 1). Fig. 1 shows the phase composition and proportion of LS and G measured by quantitative X-ray diffraction (Q-XRD) using TiO_2 (10–13 wt%) as an internal standard. The mechanism and reactions involved in forming ettringite were detailed in [2,18], in which ettringite was the main crystalline phase. This study used quartz standard sand, complying with EN 196 [19], as an aggregate to produce mortar samples; the specific grain size distribution ranges between 0.08 and 2 mm.

Citric acid (commercial product C1949 supplied by Tokyo Chemical Industry Co., Ltd., Japan) was used in this study. The acid was categorized as a retarder for OPC systems according to ASTM C494 [21]. Despite the effectiveness of citric acid as a retarder in ettringite-based binders [11,12], the mechanism is not yet clear. As discussed in [16], the acid prevents ettringite's nucleation and subsequent crystal formation. On the other hand, the authors of [22] suggested that the acid retards the hydration of OPC not by complex formation, but via the reduction in dissolution of clinker grains.

Table 1
Chemical composition (wt%) of LS and gypsum measured by XRF.

Oxide	CaO	SiO_2	Al_2O_3	Fe_2O_3	MgO	SO_3	TiO_2	LOI[a]	Others
LS	50.6	13.9	24.4	0.4	3.8	0.4	4.1	1	1.4
Gypsum	32.3	0.7	0.1	0.1	0.4	42.0	–	21.3	3.1

[a] Loss on ignition at 950 °C according to EN 196-2 [20].

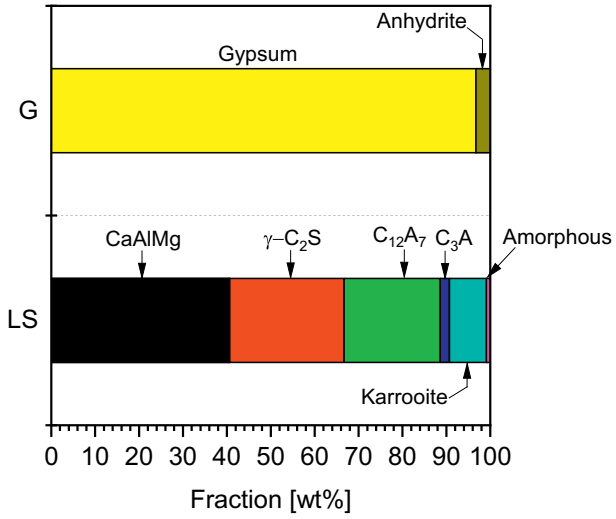

Fig. 1. The phase composition in LS and G measured by Q-XRD.

2.2. Experimental features and procedures

2.2.1. Fresh-state properties

The setting time was determined using an automated Vicat apparatus (model E044N by Matest, Italy) at room temperature according to EN196 [19] for paste samples. The paste samples were poured into a plastic conical mold on a glass substrate. The needle was set to take a measurement every 1 min until the final setting time was obtained. Table 2 shows the mixture composition and proportion of LSG mortar samples.

Heat evolution during activation was observed with isothermal conduction calorimetry (TAM Air Instruments) at 25 °C (Fig. S1). Paste samples were mixed ex situ and poured into glass ampoules before placing them into the TAM Air calorimeter; the sample mass was noted for further calculations. To minimize factors that can affect the measurement as reported in [23], all paste samples ranged from 30 to 38 g, and there were only 3 out of 8 channels used in the calorimeter at once. The baseline of the heat flow signal was determined prior to injecting glass ampoules into the isothermal instrument. The heat flow signal was recorded automatically every second for a total of 400 h for further analysis.

In situ XRD data were collected with a D2 PHASER (Bruker) automated diffractometer with Cu-K_α radiation and equipped with Lynx-eye super speed position sensitive detector. The X-ray tube was operated at 30 kV and 10 mA. After mixing the paste for 3 min, the paste samples were placed into the sample holder, and the surface was smoothed. To prevent water evaporation and carbonation, the sample was sealed with Kapton polyimide foil. The measurements were conducted at room temperature from 6 to 55° 2θ with a step size of 0.02° and a counting time of 0.3 s/step. This resulted in a total of 103 diffraction patterns collected at time intervals of 13 min. Qualitative analysis was performed with EVA V.3.1 (Bruker AXS). The MAUD program [24,25] based on the Rietveld method [26] was applied for quantitative determination of the crystalline phases. These quantification results

Table 2
Mix proportions (by mass) of the LSG with different citric acid concentrations.

Material	Slag	Gypsum	Sand	W/B[a]	Citric acid[b]
LSG	0.7	0.3	3	0.45	

[a] The W/B (water-to-binder ratio) with the total binder mass was determined by summing the mass of the slag and the gypsum.
[b] The citric acid was mixed with water to produce a solution with a targeted concentration. There were 5 different acid concentration in range 0–2 wt%.

reflect the mean phase composition over a period of 13 min. The phase contents (W) of gypsum and ettringite were derived from the refined Rietveld scale factors and were calculated from the changes of the scale factors starting from a known initial maximum content of gypsum as a precursor (i.e., 30 wt%) according to Eq. (1) [27,28], where S_t and S_{max} are the scale factors at a given time and at the beginning, respectively:

$$W = \frac{S_t}{S_{max}} \times 30 \quad (1)$$

2.2.2. Hardened-state properties

For the phase characterization, all the mixtures were characterized by different analyses to distinguish their mineralogy. Ex situ XRD analysis was performed using Rigaku SmartLab 9 kW. Identification and quantification of crystalline phases was performed in the range of 5–120° 2θ using 0.02°/step with Cu Kα radiation (Kα1 = 1.78892 Å; Kα2 = 1.79278 Å; Kα1/Kα2 = 0.5). XRD analyses were performed on paste samples at 1 and 28 days. Phase identification was done using X'pert HighScore Plus (PANalytical software). TiO2 (10–13 wt%) was used as an internal standard for quantitative analysis of the ground LSG pastes at 28 days of hydration. It is worth noting that XRD patterns shown in this study are for samples without the internal standard for better visualization of crystalline phases in LSG.

The ^{27}Al MAS NMR spectra were obtained with the help of a Bruker Avance III 300 spectrometer operating at 78.24 MHz for ^{27}Al. The paste samples were packed into 7 mm zirconia rotors, and a spinning frequency of 7 kHz was applied; 2048 scans were accumulated with a repetition rate of 2 s. Neither proton decoupling nor cross polarization was used. $Al(NO_3)_3$ was used for the purpose of referencing; its chemical shifts were set to zero ppm. The ^{27}Al MAS-NMR spectrum was deconvoluted into Gaussian components representing reactant species and hydrations products (ettringite, monosulfate, and aluminum hydroxide) using Origin software. Deconvolution involved assuming the isotropic chemical shift (± 0.5 ppm) for each phase from the literature as well optimizing the NMR spectra parameters like signal intensity and full width at half maximum (FWHM). The deconvolution process was satisfactory to the extent that the R^2 value obtained was at least 0.98. The errors in areas of various components were obtained from the output parameters after deconvolution using the Origin software. The chemical shift values used for various product components during the deconvolution are listed in Table 3. Note that the reactant portion was deconvoluted into three components, and no phase assignment was conducted for these components—they were just used to estimate the total reactant phases remaining in the binders.

In terms of the mechanical testing, the compressive strength of LSG mortars at different percentages of citric acid was measured. The mortar samples were prepared according to EN-196 [19]. LS and gypsum were initially blended for 3 min, after which the citric acid solution and sand were added in a 5 L mixer at low (roughly 70 rpm) and high (roughly 150 rpm) speeds. The mortar samples were cast into 40 × 40 × 160 mm^3 molds and vibrated for 2 min at a frequency of 1 Hz. The samples were cured in plastic bags at room temperature for 24 h before demolding and then in a water bath at room temperature (approximately 23 °C) until testing. The compressive strength tests were conducted after 7 and 28 days of curing. The compressive strength was measured by loading the halves of the prismatic specimens via a Zwick Z100 or a Dartec with a load cell of 100 or 400 kN, respectively. At least four specimens were tested for each mixture, and the displacement was controlled at 1 mm/min.

Table 3
Chemical shifts for the NMR spectra deconvolution of various Al-containing phases.

Phases	Chemical shift [ppm]	References
Ettringite	13.0	Skibsted et al. [29]
Monosulfate	9.0	Skibsted et al. [29]
Aluminum hydroxide	5.0	Rottstegge et al. [30]
Reactants	52.7; 58.9; 68.7	–

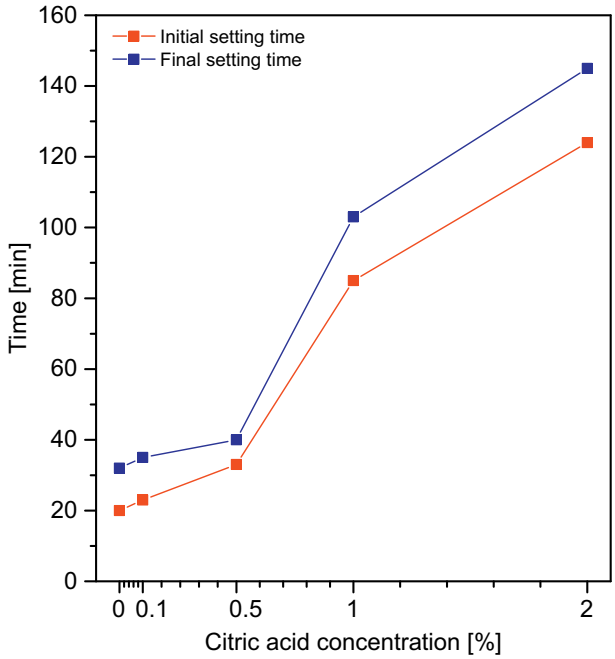

Fig. 2. The initial and final setting times of LSG paste with different percentages of citric acid; for a comparison, Portland cement usually has initial setting time in a range of 60–180 min.

3. Results and discussion

3.1. Fresh-state properties

3.1.1. Setting time

The citric acid exhibited a retardant effect when the dosage ranged from 1 to 2 wt% solution. Fig. 2 shows the initial and final setting time of the mixtures using different amounts of citric acid in comparison to the plain mixture (without citric acid). The acid prolonged the initial setting time by approximately 4 and 6 times when 1 and 2 wt% citric acid was used, respectively. As for the final setting time, the citric acid at a concentration of 1 and 2 wt% offered an increase of roughly 3.2 and 4.5 times, respectively, to the LSG plain paste. In [12], the acid was reported to slow down the production of ettringite in a ternary system Portland cement–calcium sulfoaluminate clinker–anhydrite. As a type-B retarder for OPC [21], the acid reduced hydration kinetics significantly at a dose of 0.4–0.5 wt% cement [22].

In contrast, the citric acid seemed to have negligible effects when used at lower doses compared to higher ones (≥1%). The initial and final setting times of the LSG paste slightly increased by a maximum of 65% and 25%, respectively, when a 0.5 wt% citric acid solution was used. However, the samples set much faster than that of the 1–2 wt% citric acid solution (Fig. 2). In [22,31], the authors reported that the addition of small amounts of citric acid (0.1 wt% binder) slightly accelerated the hydration of aluminate and the formation of ettringite, while the addition of citrate strongly retarded ettringite formation as the dosages increased to 0.2–0.5 wt% binder. In [12], when the citric acid content was low (0.27 wt% to the binder), it could affect the early formation rate of ettringite; however, once all the citrate ions would have been complexed, the formation rate would have accelerated.

3.1.2. Heat of hydration

The presence of citric acid in mixtures reduced the peak of the heat

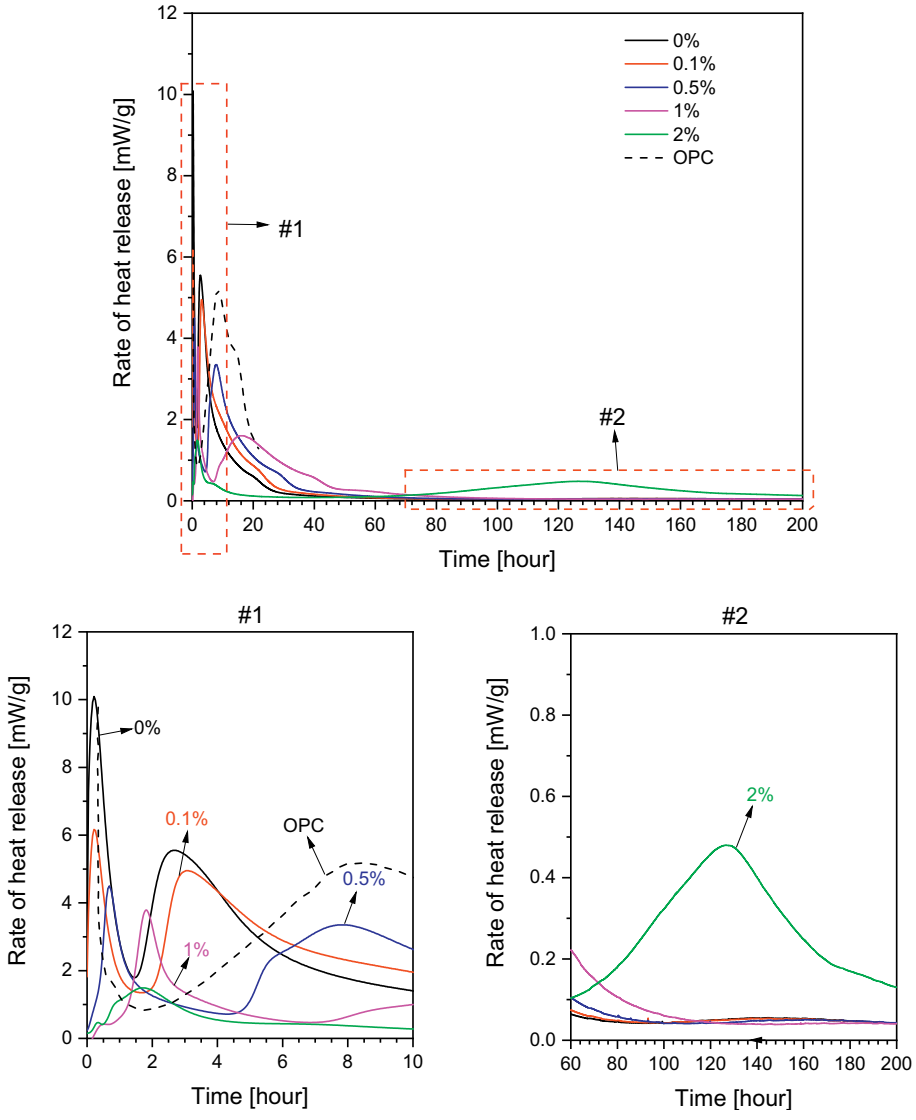

a)

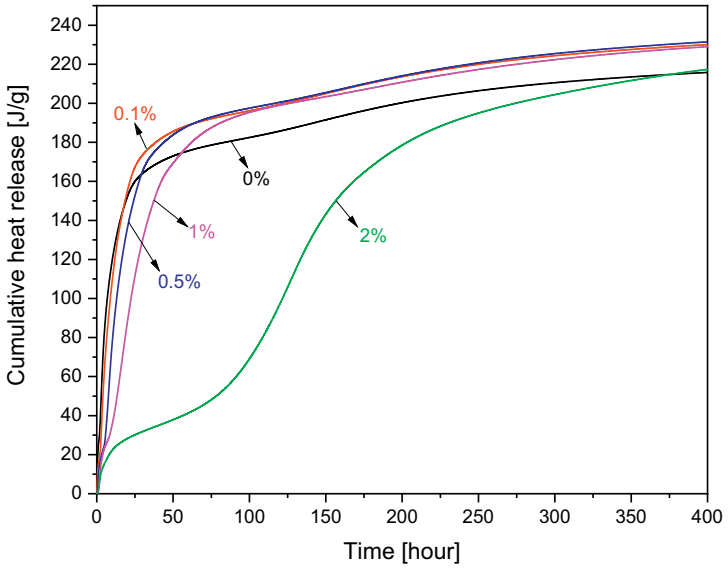

(b)

(caption on next page)

Fig. 3. The heat of hydration measured by isothermal calorimetry, including (a) the rate of heat release (with magnifications #1 and #2), and (b) the cumulative heat release of LSG pastes with different citric acid concentrations; data for the heat evolution of OPC was adopted from Jansen et al. [32].

release and shifted the peak evolution to a longer time. Fig. 3a shows the heat evolution of mixtures until 200 h after the reaction started according to Eqs. (2)(4). Increasing the concentration of citric acid in the mixtures significantly reduced the maximum heat (see Fig. 3a, #1); the first peak was shifted to approximately 2 h with the presence of 1 wt % citric acid solution. In addition, the peak seemed to broaden when the amount of citric acid was increased. It is worth mentioning that the initial peak is attributed to the wetting and dissolution of LS and rapid hydration to form ettringite [13]. The initial peak was distinguished from the other samples, showing that the appearance of the acid in the mixtures strongly retarded the hydration of LSG. A similar observation with delayed and broadened peaks was reported in [33]; it featured a 0.2 wt% sodium citrate used as a retarder. In addition, the dissolution of the calcium aluminate crystal phases (i.e., likely C_3A), the resorption of sulfate ions from C_3A surfaces, and accelerated ettringite precipitation in the binder could create a shoulder on the deceleration peak [34], which was observed on the LSG with a 0.5–2 wt% citric acid solution, whereas the lower content of the acid did not exhibit this shoulder (see Fig. 3); a similar evolution in OPC system was reported in [34].

$$C_{12}A_7 + 12C\bar{S}\bullet 2H + 137H \rightarrow 4C_3A\bullet 3C\bar{S}\bullet 32H + 3AH_3 \quad (2)$$

$$C_{12}A_7 + 4C\bar{S}\bullet 2H + 49H \rightarrow 4C_4A\bar{S}H_{12} + 3AH_3 \quad (3)$$

$$C_3A\bullet 3C\bar{S}\bullet 32H \leftrightarrow C_4A\bar{S}H_{12} + 2C\bar{S}H_2 + 16H \quad (4)$$

The hydration kinetics of LSG observed via heat evolution was, however, different among the mixtures. It varied from roughly 30 h for the plain mixture to 180 h with a 2 wt% citric acid solution (see Fig. 3a, #2). In addition, as shown in Fig. 3a, the dormant period after the initial peak was prolonged when the amount of citric acid was increased (e.g., up to roughly 70 h with a 2 wt% citric acid solution). Furthermore, the citric acid had a more dominant effect on this dormant period than on the initial peak heat (as shown in Fig. 4a). On one hand, the initial peak was just slightly delayed when the citric acid content was increased. On the other hand, the time before the initiation of the second peak heat was significantly prolonged when the citric acid content was increased. As discussed in [22,35], the citrate retardation might be attributed to the reduction in the precursors' dissolution rate. However, the mechanism could be a complex formation on the anhydrous cement surface [35]—or it could not [22]. It is worth noting that the mentioned work investigated an OPC system; however, the effects of citric acid on the dissolution of calcium in Al-rich phases might contribute to the retardant effects seen in [13].

The cumulative heat released after 400 h of hydration (Fig. 3b) shows that mixtures with 0.1–1 wt% citric acid solution had comparable total heat release, while the plain and LSG with 2 wt% citric acid attained slightly lower value. After the first 100 h, the mixture with a 2 wt% citric acid solution produced the least cumulative heat in comparison to the other mixtures. However, after > 2 weeks of hydration (around 400 h), the total heat of the mixture was roughly the same as that of the plain mixture due to the delay in the hydration. In addition, the mixtures with a 0.1–1 wt% citric acid solution attained a slightly higher heat release than the plain LSG. This may be due to the effects of citric acid on promoting hydrations inside the cementitious binder under its chelation. This effect probably plays an important role in the strength development of the material at a later age. Additionally, since the result of cumulative heat release was recorded until 16 days of hydration, there was no data to consider the total heat in LSG with 2 wt % citric acid solution at final age (28 days) correlating with its strength.

The correlation between the setting time and the initial peak heat evolution was found via a quadratic function (Fig. 4b). Both the initial and final setting times were in good agreement with the heat evolution. Interestingly, the OPC system showed very little relationship between heat evolution and setting time, as reported in [36], due to several exothermic reactions occurring simultaneously in the OPC [32]. In contrast, in ettringite-based binders, the microstructure building the reaction in the system is the only important reaction taking place in the early ages [13]. In addition, the final setting time obtained a slightly higher correlation with the time to the peak heat evolution than it did the initial setting time. This behavior is in line with the calcium sulfoaluminate cements reported in [13]. Also, the correlation is very

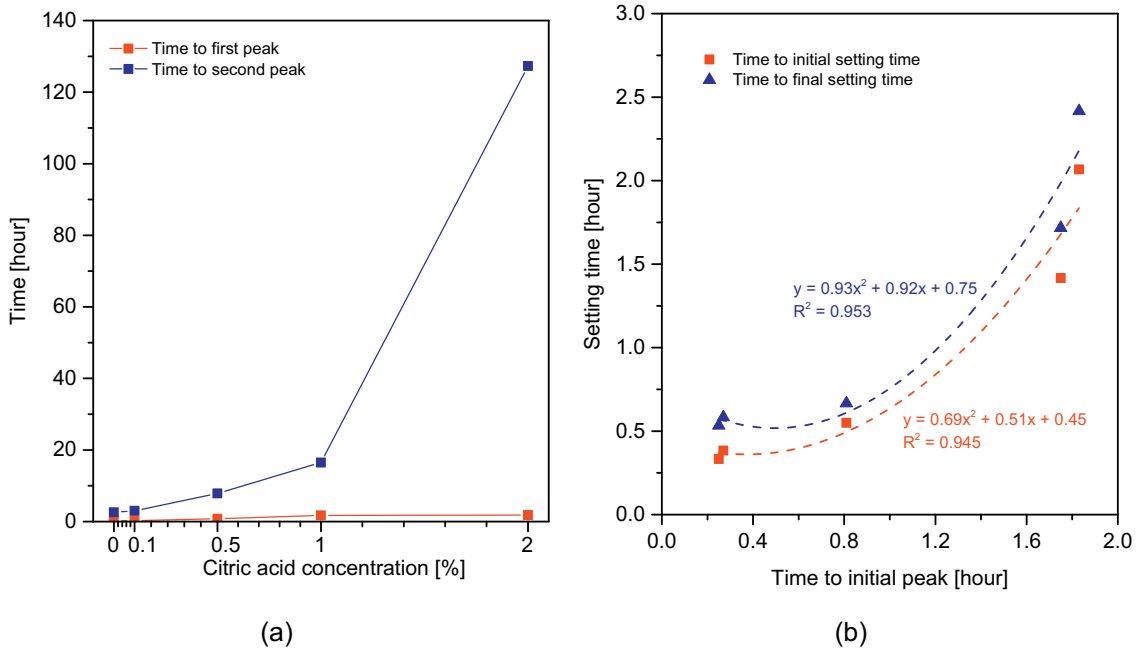

Fig. 4. (a) The relationship between the first/second peak in the heat evolution and the citric acid concentration, and (b) the correlation between the initial/final setting time and the first peak of the heat evolution.

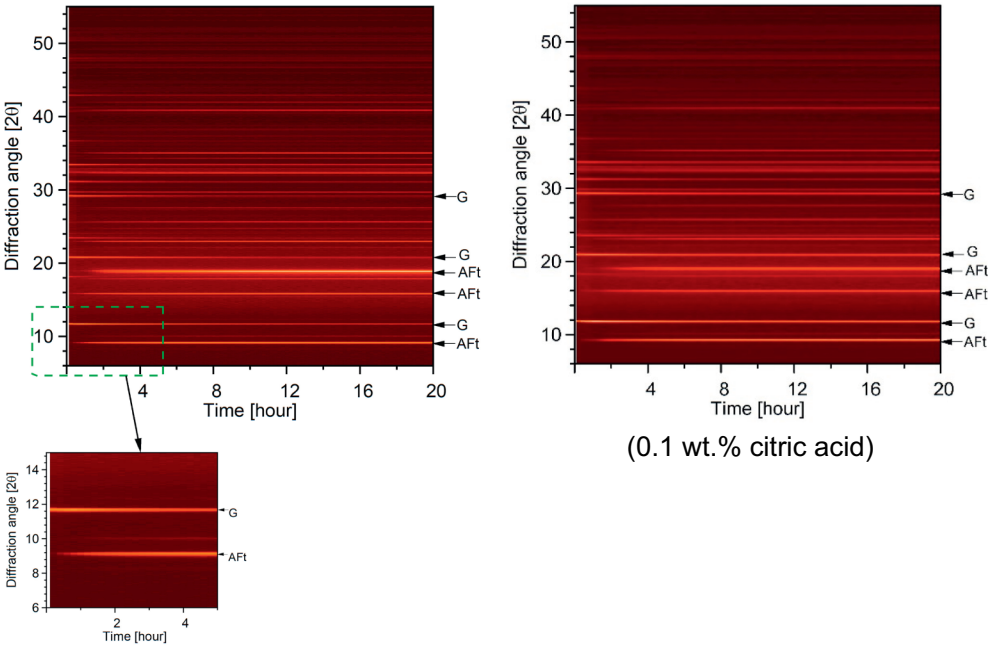

(0 wt.% citric acid) (0.1 wt.% citric acid)

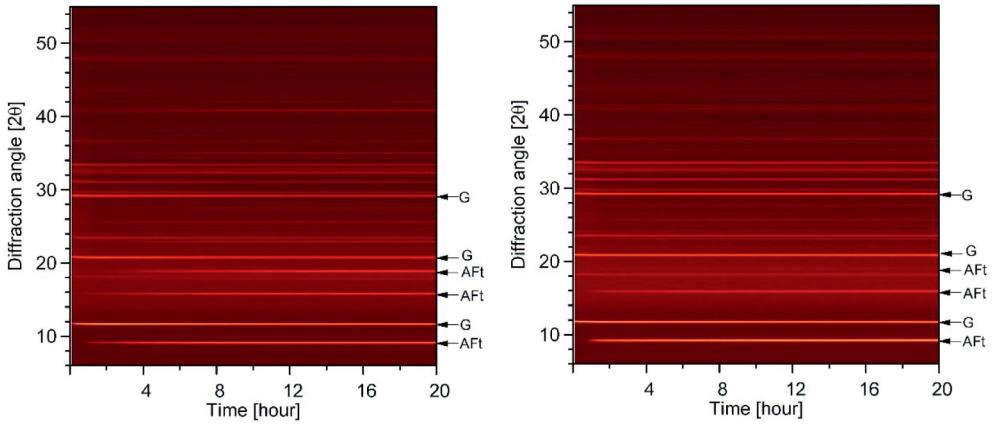

(0.5 wt.% citric acid) (1 wt.% citric acid)

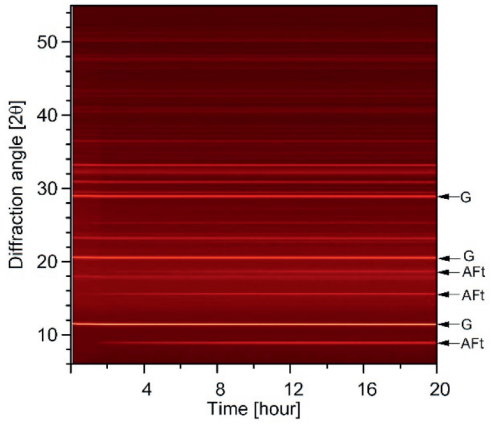

(2 wt.% citric acid)

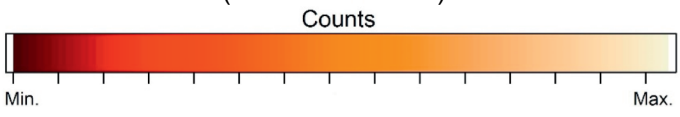

(caption on next page)

Fig. 5. In situ XRD characterization of LSG pastes in the first 20 h (approximately 100 scanning times) of LSG hydration with the considered contents of the citric acid solution; the measurement was conducted after every 13 min with ettringite (AFt) and gypsum (G).

helpful in terms of predicting the setting time of citric acid dosages and their heat evolution results.

3.1.3. In situ XRD

There was a trace of ettringite detected at the beginning of the hydration of plain LSG, whereas the citric acid delayed formation of ettringite (as shown in Fig. 5). It can be seen that during the first measurements of in situ XRD, the appearance of ettringite (AFt) was already detected in the LSG paste without citric acid; XRD reflexes of AFt are visible after 13 min, when the first measurement was taken. The reflexes of the ettringite peaks (e.g., at 2θ of roughly 9.5° and 19°) kept increasing rapidly in the first 10 h of hydration and became stable at the end of the measurement. This shows the fast formation of ettringite in the LSG mixture, which is similar to other ettringite-based binders that precipitated ettringite within the first 24 h of hydration [37,38]. In contrast, the citric acid clearly had retardant effects on the formation of ettringite, especially at a high dosage (e.g., a 2 wt% solution). The 2 wt% citric acid solution contained in Fig. 5 shows the traces of ettringite beginning approximately 2 h after hydration in LSG. In contrast, the LSG mixture with a 0.1 wt% solution seemed to have no delay in the formation of ettringite, thus exhibiting the rapid setting property reported in Section 3.1.1. It is worth noting that after 20 h of in situ XRD measurement, there was still gypsum left in all the hardened pastes; hence, further reactions might continue after this period. In addition, the presence of amorphous phase, formed from the hydration of LSG, at early age was not clearly shown in the in situ XRD results since the hump between around 12° to 25° (i.e., the light-red-colored area in the in situ XRD maps) was mainly due to the presence of Kapton foil and water attributed to the XRD patterns. Fig. S2 shows the evidence of the contribution of Kapton foil and water to the aforementioned hump.

Fig. 6 shows the results of the quantitative phase determination of the in situ XRD measurements combined with the heat evolution from the isothermal calorimetry conducted on the LSG pastes. Without citric acid (Fig. 6a), ettringite formed rapidly from the reaction between $C_{12}A_7$ and gypsum, leading to the initial peak of the heat release. The reaction continued in the steady-state region (roughly 1.5 h of hydration). The decrease in heat release might be due to the transformation from non-crystalline to crystalline ettringite [39]. Other studies discussed this reduction in the rate of heat release caused by the transformation of ettringite into monosulfate at an early age [40,41]. However, it is hard to detect monosulfate at this stage with XRD because the phase has a poor crystallization degree at early-age hydration [41]. The second peak of the heat evolution was attributed to the ettringite formation, and it is in good agreement with the quick consumption of $C_{12}A_7$, gypsum, and the presence of ettringite in the phase content of the quantitative in situ XRD results. The reaction reached the stable stage after roughly 10 h of hydration; here, the heat release significantly decreased, and ettringite became the dominant highly crystalline phase in the binder.

The hydration kinetics of LSG were reduced with the presence of citric acid. As shown in Fig. 6b, the initial peak of heat evolution was roughly at 2 h, while the ettringite slowly began its formation at that time. The reaction continued until the percentage of ettringite reached approximately 10 wt% of the total binder mass after 14 h. The hydration kinetics were much lower than that of the LSG paste without citric acid. Hence, after the same amount of time, this proportion of ettringite in LSG with 2 wt% citric acid was much smaller than the one without citric acid; it was in agreement with the cumulative heat release of the samples (Fig. 3b). Furthermore, the heat evolution in Fig. 3a shows the second peak of the sample after approximately 5 days of hydration, which was attributed to the second ettringite formation. With a very long induction period, the formation of ettringite was delayed, likely promoting the transformation from ettringite to monosulfate. Additionally, at the end of the in situ XRD measurements, the total proportion of crystalline phases in LSG without and with a 2 wt% citric acid solution was around 54% and 49%, respectively. This means that there was a large percentage of amorphous phases (roughly 50%) in the binder attributed to AH_3, monosulfate, and unreacted phases.

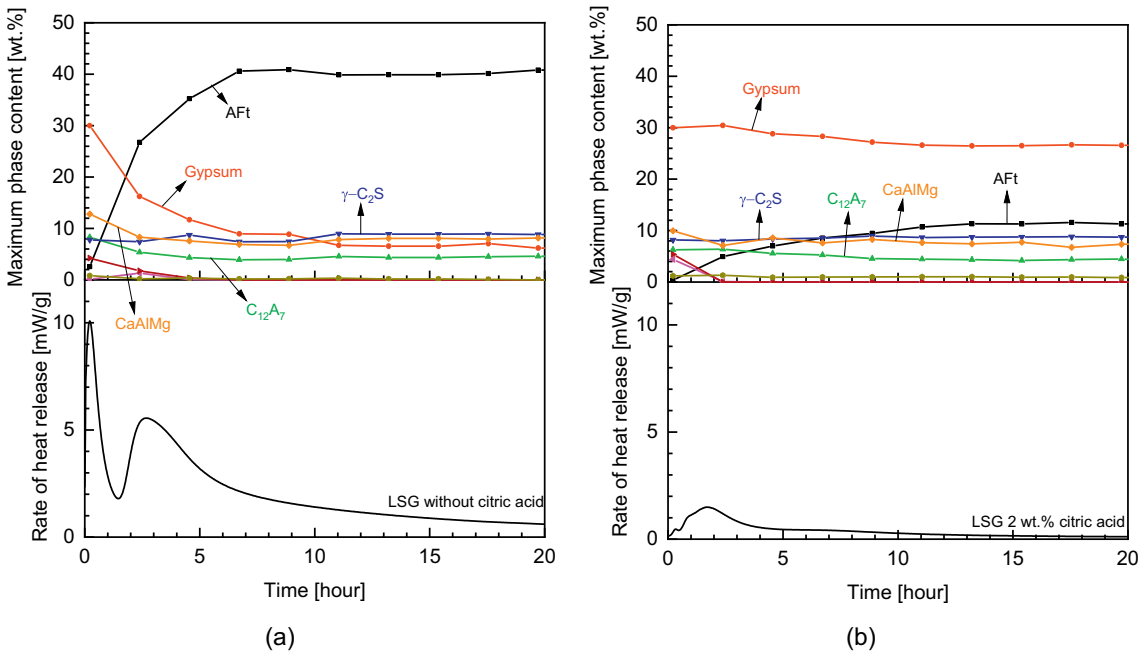

Fig. 6. Crystalline phase evolution from quantitative in situ XRD and heat flow curve during the reaction of LSG paste with (a) a 0 wt%, and (b) a 2 wt% citric acid solution (graphs of LSG with other citric acid concentrations can be found in the Supplementary data of this article).

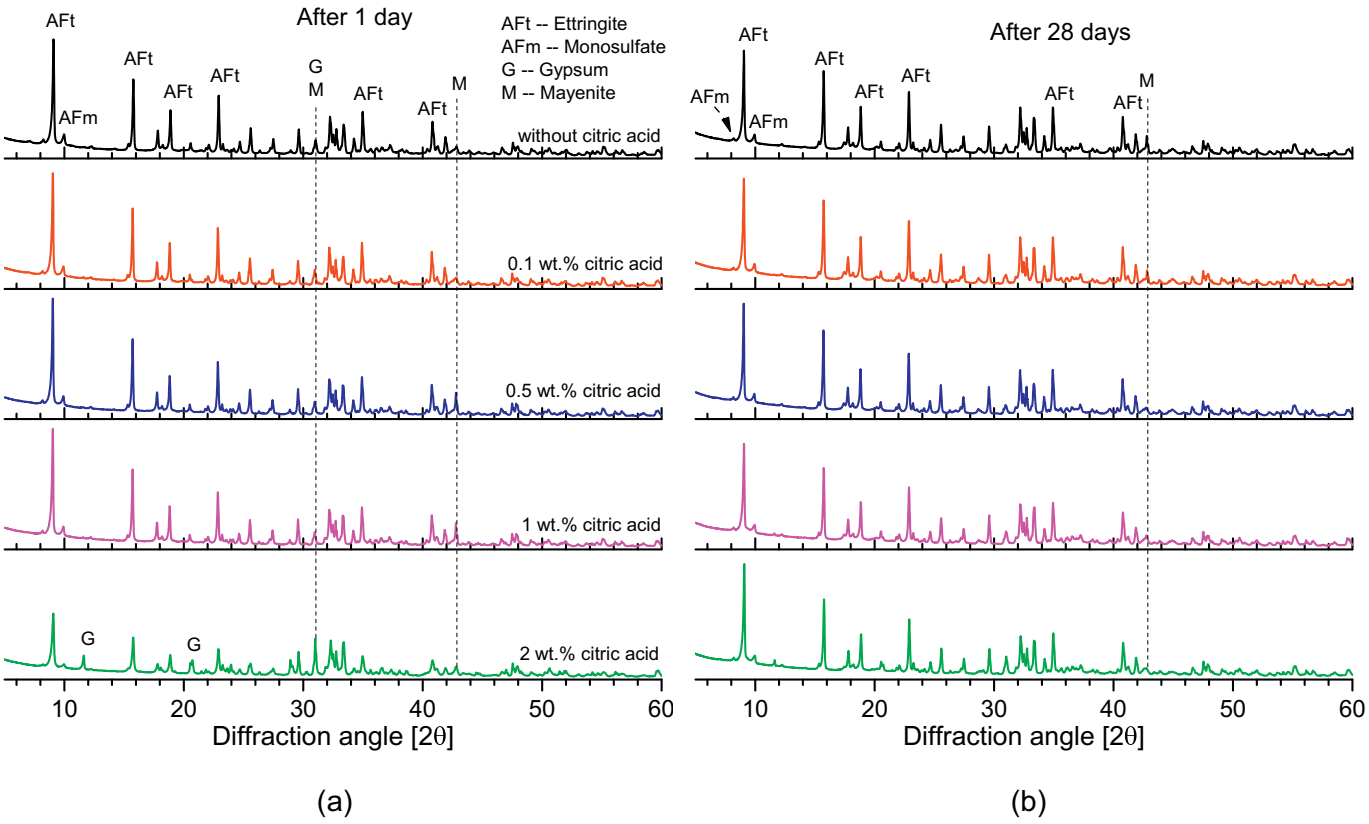

Fig. 7. Ex situ XRD characterization of LSG pastes after (a) 1 day, and (b) 28 days of curing.

3.2. Hardened-state properties

3.2.1. Phase characterization

Ettringite was a dominant crystalline phase, and there was a trace of monosulfate in all the LSG mixtures with different citric acid contents at both early and late ages. The quantitative results from the XRD reported in [2] showed that ettringite might occur at approximately 35% in LSG, resulting from the reaction listed in Eq. (2). In contrast, the monosulfate trace was detected in the ex situ XRD, as shown in Fig. 7. It can be seen that monosulfate formed at a very early age (1 day of hydration); this behavior has been reported in previous literature [40–42]. The formation of monosulfate could be due to either of two reasons. First, when sulfate, calcium ions, and water content are insufficient in a solution, $C_{12}A_7$ may hydrate with gypsum (according to Eq. (3)) to produce monosulfate; this reaction was reported to happen at a very early stage of the reaction, which can be seen in the induction period of the heat evolution reaction [41,43]. Second, it is possible for ettringite to convert to monosulfate (Eq. (4)); the reverse reaction may occur during the self-desiccation stage of the hydration [41]. In addition, monosulfate's stability has been reported to be strongly dependent on its surrounding environment—namely, the characterization of the pore solution, the amount of water, and the pH conditions. These factors affect the stability equilibria and modify the composition and structure of the monosulfate [44]. Moreover, as reported in [12], monosulfate is thermodynamically favored, and the content of this crystal tends to increase in ettringite-based binders.

The Q-XRD results in Fig. 8 confirms the phase composition of all mixtures with different citric acid concentration. In Fig. 1, it can be seen that the raw LS contains minor amount of amorphous (roughly 3 wt%). As found in [45] for super sulfated slag cement, the amount of amorphous phase slags is less important for the reactivity than its optimum chemical composition. In contrast, the amorphous ranges from 25 to 35 wt% in LSGs with different citric acid content, which is likely due to

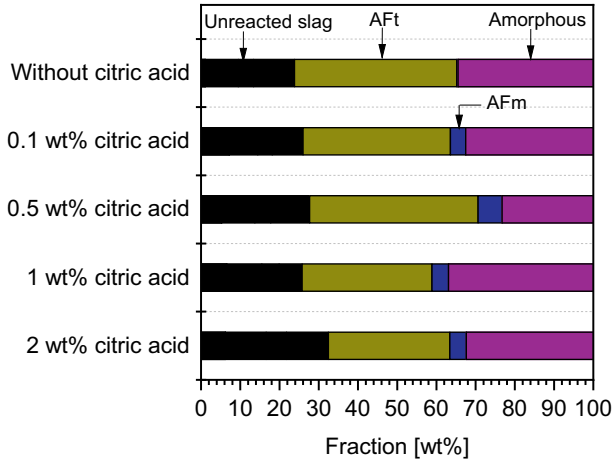

Fig. 8. The phase quantification of LSG with different citric acid content after 28 days of hydration.

the formation of C-S-H, low-crystallinity AFm phase (e.g., monosulfate and solid solution AFm), and AH3. In addition, ettringite is also found to be the main crystalline phase in the binder with a fraction of 33–40 wt% in LSG.

Solid-state ^{27}Al MAS NMR analysis suggests the existence of AFm in the structure of all the LSG paste mixtures at both the early and final ages (Fig. 9). There were three main Al-containing hydration phases, as indicated by the reactions in Eqs. (2)(4): ettringite, monosulfate, and aluminum hydroxide. In addition, the leftover reactant was also detected in both the 1- and 28-day samples. It can be seen that ettringite was the well-crystalline phase that exhibited a relatively narrow peak (a small FWHM) at a chemical shift of roughly 13.0 ppm. In contrast, AFm including monosulfate was a semi-ordered Al-containing phase; hence,

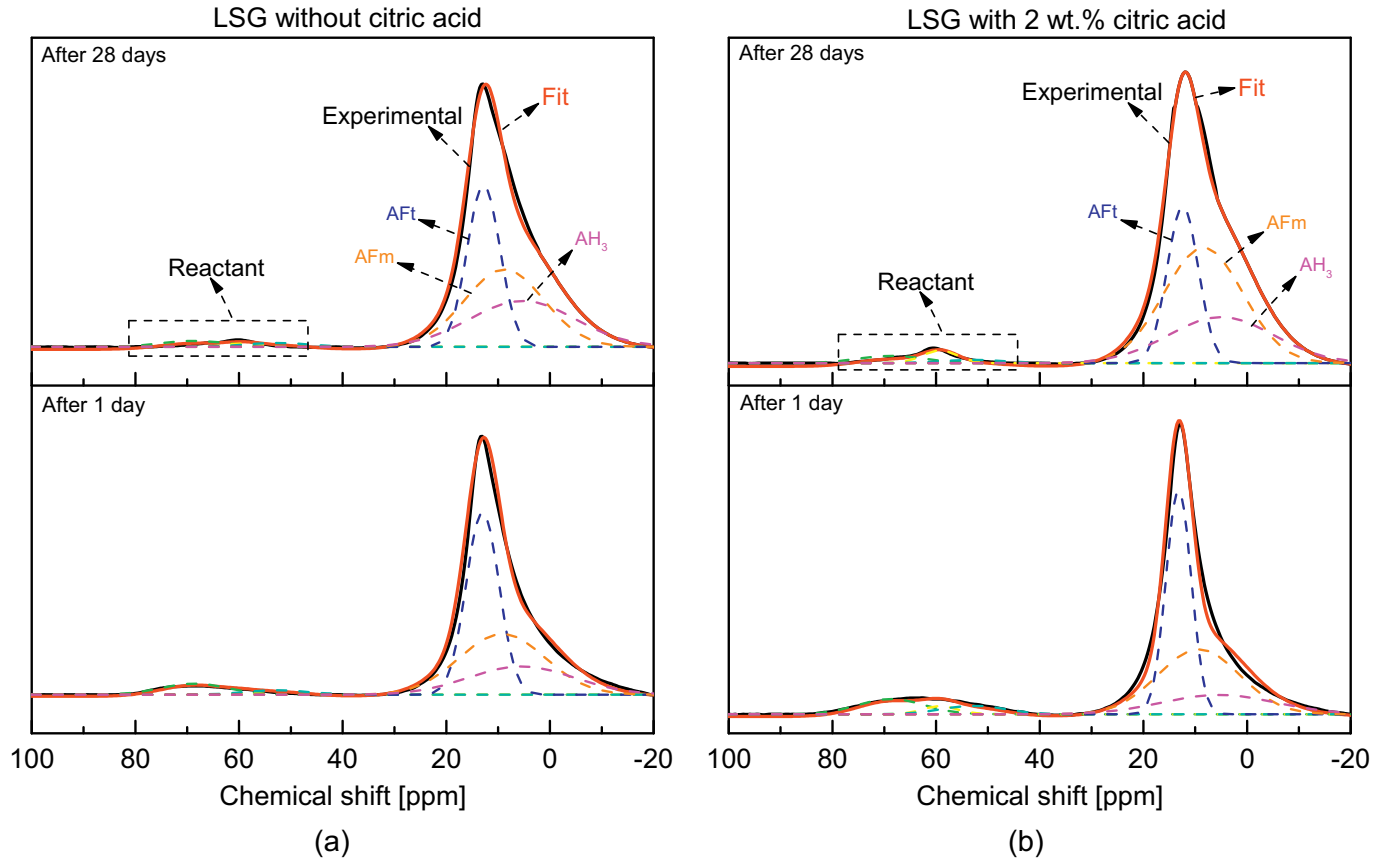

Fig. 9. Deconvolution of ^{27}Al MAS NMR spectra of LSG paste with (a) 0 wt%, and (b) 2 wt% citric acid solution after 1 and 28 days of age (graphs of LSG with other citric acid concentration can be found in the Supplementary data of this article).

it attained a broader peak (a large FWHM) at around 9.0 ppm [29,46]. This is why it was hard to detect the phase in both the in and ex situ XRD (Figs. 4 and 6). However, both the XRD and NMR results showed the appearance of AFm at a very early stage of the hydration regardless of the citric acid content. Regarding the aluminum hydroxide phase, the broadness of the peak proved its amorphous nature. The role of aluminum hydroxide needs more understanding, as the gel offered high indentation modulus and hardness and could improve the density of hardened mortar [47,48].

Based on the quantitative results for LSG from NMR analysis, citric acid promoted the conversion from ettringite to monosulfate in the LSG binder. Fig. 10 shows the quantification of various Al phases in LSG with different citric acid contents and the development trend of these phases at 1 and 28 days. The fraction of ettringite in total Al-contained phases was similar in all mixtures after 1 day of hydration, except for LSG with a 2 wt% citric acid solution. This was due to the retardant effects of the acid that delayed the formation of ettringite at early age as shown also in Fig. 6b. The conversion from ettringite to monosulfate was observed after 28 days, in which the fraction of ettringite in LSG was reduced by approximately 10–15% (Fig. 10a). In addition, the conversion rate from ettringite to monosulfate and the citric acid content had a proportional relationship (Fig. 10a and b). This is due to the retardant effects of citric acid, which delay the dissolution of calcium along with the reduction of the water content that promoted the reaction in Eq. (3). In contrast, monosulfate occurred in a similar fraction with ettringite at an early age (i.e., roughly 30%); this result conflicts with the XRD results reported previously due to monosulfate's poorly ordered crystalline structure [46,47], which led to difficulties in detecting the phase using XRD. Regarding aluminum hydroxide, the phase slightly increased after 28 days of hydration, meaning that a further reaction occurred; it can be seen that Eqs. (2)(4) all formed aluminum hydroxide as a minor hydration product.

3.2.2. Compressive strength

The compressive strength of LSG attained the highest increase at an early age with a citric acid concentration of 1 wt%. The compressive strength increased slightly by a maximum of around 20% with a 1 wt% citric acid solution used after 7 days of curing (Fig. 11a). In contrast, when the higher dosage of citric acid was used (i.e., 2 wt% solution), the strength was reduced by approximately 14% compared to LSG with a 1 wt% solution. This is due to the presence of citric acid in the mixture, which prolonged the hydration process to form strength-giving phases in LSG. In contrast, the increment was not significant with lower dosages (0.1 and 0.5 wt% solution); this might be attributed to the accelerating effects of citric acid on the calcium aluminate system, as observed in the setting time tests.

At the final age, and when used in high dosages, the citric acid exhibited very positive influences on the development of the LSG mixtures' compressive strength, increasing significantly by a maximum of 45% with a 2 wt% citric acid solution (Fig. 11a). Additionally, the presence of citric acid offered an improvement in the LSG's compressive strength beginning with a dosage of a 0.5 wt% citric acid solution, whereas the lower dosage seemed to have no effect even after a longer curing time. Interestingly, the compressive strength of LSG with a 2 wt % citric acid solution was enhanced by 35% between its early and final age. This is due to the formation of hydration products at a later age probably caused by the effects of citric acid in reducing the reactants' dissolution rate. This result is in good agreement with the heat evolution shown in Fig. 3. The second peak of the LSG mixture with the highest citric acid content shifted after 5–7 days of hydration; hence, the strength significantly improved at the final age (as shown in Fig. 11a). In addition, it seems that the monosulfate contributed to the

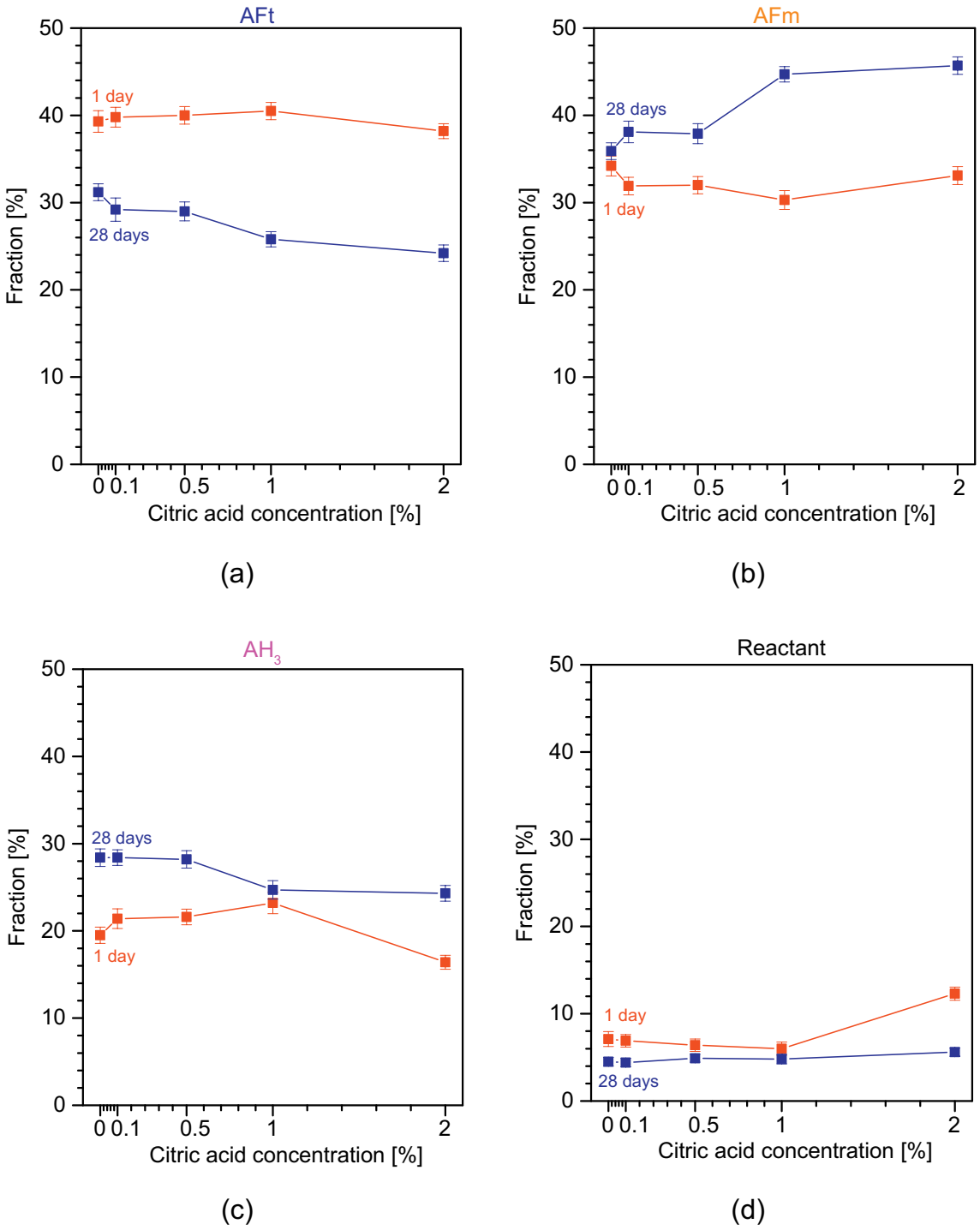

Fig. 10. Quantification of various Al phases obtained through the deconvolution of ^{27}Al MAS NMR spectra: (a) ettringite, (b) monosulfate, (c) aluminum hydroxide, and (d) the leftover reactant in different citric acid concentrations after 7 and 28 days of age.

strength increase of the LSG, as the strongest mixture (a 2 wt% citric acid solution) contained the highest amount of monosulfate (see Fig. 10b). In contrast, the plain LSG attained roughly 50 MPa in compressive strength after 7 days and had no development in strength later on. Therefore, the citric acid offered not only the set retardant effects but also the positive influences on the strength development of the LSG mortar. In [13], the authors reported no negative effects from citric acid when it was used in different types of commercial calcium sulfoaluminate cements. Moreover, the plain LSG mixture obtained a very good compressive strength and met the requirements for high early-strength cement according to ASTM C1600 [49]. Hence, by using citric acid, the setting time and compressive strength of LSG at both early and later ages can be optimized and controlled based on this binder's uses in construction. Moreover, the effect of citric acid on the porosity of LSG binder is suggested as a future investigation.

Fig. 11b shows a correlation between the initial peak of the heat evolution and the LSG's compressive strength with different citric acid concentrations after 28 days. The LSG's compressive strength and the heat evolution have a linear relationship with a high correlation coefficient. This relationship indicates that the later the initial peak heat

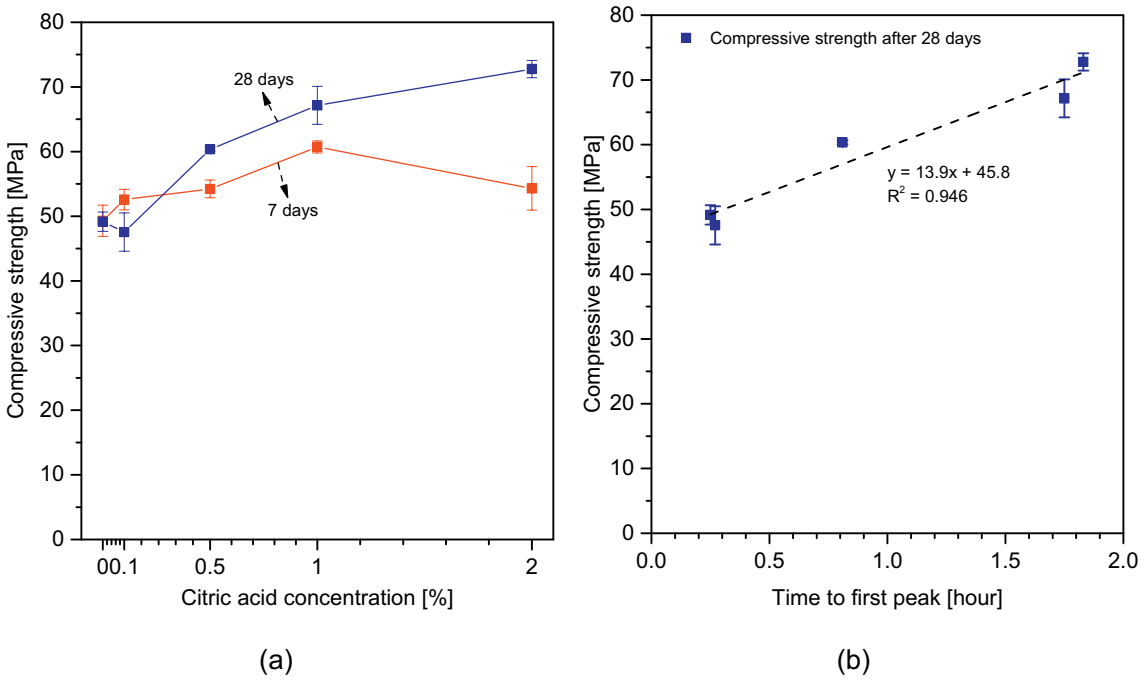

Fig. 11. (a) Compressive strength at 7 and 28 days of LSG mortars with different citric acid concentrations (average and standard deviation of four tests), and (b) correlation between the first peak of the heat evolution and the compressive strength after 28 days.

appeared, the higher the compressive strength of the LSG. In addition, if the hydration happens too quickly, this can lead to lower strength at a later age as seen in LSG without citric acid. It is worth noting that the LSG's compressive strength did not have a good correlation with the second peak of the heat evolution. This may be due to citric acid's strong retardant effects at an early age, which lead to LSG's late strength development (i.e., LSG with a 2 wt% citric acid solution). In addition, as shown in Fig. S5 (Supplementary data), there was no clear correlation between compressive strength and cumulative heat of LSG samples at 7 days. More research data are needed to confirm the relation between the 2 parameters in LSG binders.

4. Conclusions

This experimental investigation studied the retardant effects of citric acid produced from the hydration between ladle slag and gypsum on an ettringite-based binder (LSG). The acid works as an effective set retarder at relatively high dosages (i.e., a 1–2 wt% solution), while there are no clear effects at lower dosages (i.e., a 0.1–0.5 wt% solution). Therefore, by using citric acid at different contents, the setting time and the workability of the ettringite-based binder can be controlled; the applications of this binder can be broadened to various fields of construction.

Citric acid delays the formation of ettringite, as observed via the heat evolution of hydration and in situ XRD measurements. The presence of the acid in LSG pastes decreased and broadened the peak of heat evolution; it also shifted the peak evolution to a longer time. With a 2 wt% citric acid solution, the heat of hydration continued to release for up to 180 h, in comparison to the roughly 30 h of the reference LSG. However, the cumulative heat release in a period of over 2 weeks of all the mixtures was comparable to one another, meaning that citric acid retards reactions and shifts the hydration process to a later age. The in situ XRD revealed the rapid formation of ettringite in LSG paste without citric acid almost immediately after being exposed to water. In contrast, crystal formation was delayed by up to 2 h with the presence of a 2 wt% citric acid solution. Furthermore, the setting time and the initial peak heat evolution of the LSG pastes had a good correlation via a quadratic function; this can be used to predict a binder's setting time based on citric acid dosages and their heat of hydration results.

Both the XRD and solid-state ^{27}Al MAS NMR suggest the existence of AFm as one of the main hydration products of LSG. Monosulfate formed at a very early age due to the insufficiency of sulfate, calcium ions, the depletion of the water content, and the conversion from ettringite. In addition, monosulfate has a semi-ordered crystalline structure; hence, ^{27}Al MAS NMR is more favorable for quantifying the phase than is XRD. However, as a hydration product of LSG, amorphous aluminum hydroxide may play an important role in the strength development of LSG binders and needs further investigation.

At the final age, the content of citric acid and the conversion rate from ettringite to monosulfate were in a proportional relationship. This may be attributed to the delay in the calcium dissolution in the reactant as a retardant effect of the citric acid, promoting both the reaction to form monosulfate and ettringite conversion.

All the mixtures can attain a very high compressive strength at the early and final age. After 28 days of hydration, LSG with a 2 wt% citric acid solution reached its highest compressive strength (roughly 72 MPa), while the reference LSG mortar obtained approximately 50 MPa. The role of AFm phase including monosulfate contributing to the compressive strength of LSG mortar should be addressed in future studies since the strongest mortar contained the highest amount of monosulfate. In addition, C-S-H gel produced from the hydration of γ-C_2S needs more understanding, especially after a long hydration time.

Declaration of Competing Interest

The authors declare that they have no known competing financial interests or personal relationships that could have appeared to influence the work reported in this paper.

Acknowledgements

This work was done as part of the FLOW project (project number 8904/31/2017) funded by Business Finland in the ERA-MIN 2 Innovation program (EU Horizon 2020 program) and industrial partners including SSAB Europe Oy, Saint-Gobain Finland Oy, Kiertokaari Oy, and Destaclean Oy. The authors appreciate support from Prof.

Yiannis Pontikes (KU Leuven, Belgium) for in situ XRD measurements and Samppa Hyvärinen for lab work. Hoang Nguyen gratefully acknowledges financial support from the Tauno Tönning Research Foundation. A.M.K. and V.-V.T. acknowledge financial support from the Kvantum Institute (University of Oulu) and the Academy of Finland (grant numbers 289649 and 294027).

Appendix A. Supplementary data

Supplementary data to this article can be found online at https://doi.org/10.1016/j.cemconres.2019.105800.

References

[1] R.X. Magallanes-Rivera, J.I. Escalante-García, Anhydrite/hemihydrate-blast furnace slag cementitious composites: strength development and reactivity, Constr. Build. Mater. 65 (2014) 20–28, https://doi.org/10.1016/j.conbuildmat.2014.04.056.
[2] H. Nguyen, E. Adesanya, K. Ohenoja, L. Kriskova, Y. Pontikes, P. Kinnunen, M. Illikainen, Byproduct-based ettringite binder – a synergy between ladle slag and gypsum, Constr. Build. Mater. 197 (2019) 143–151, https://doi.org/10.1016/j.conbuildmat.2018.11.165.
[3] J.-M. Kim, S.-M. Choi, D. Han, Improving the mechanical properties of rapid air cooled ladle furnace slag powder by gypsum, Constr. Build. Mater. 127 (2016) 93–101, https://doi.org/10.1016/j.conbuildmat.2016.09.102.
[4] K. Quillin, Performance of belite–sulfoaluminate cements, Cem. Concr. Res. 31 (2001) 1341–1349, https://doi.org/10.1016/S0008-8846(01)00543-9.
[5] S. Peysson, J. Péra, M. Chabannet, Immobilization of heavy metals by calcium sulfoaluminate cement, Cem. Concr. Res. 35 (2005) 2261–2270, https://doi.org/10.1016/j.cemconres.2005.03.015.
[6] H. Nguyen, M. Staudacher, P. Kinnunen, V. Carvelli, M. Illikainen, Multi-fiber reinforced ettringite-based composites from industrial side streams, J. Clean. Prod. 211 (2019) 1065–1077, https://doi.org/10.1016/j.jclepro.2018.11.241.
[7] B. Ma, M. Ma, X. Shen, X. Li, X. Wu, Compatibility between a polycarboxylate superplasticizer and the belite-rich sulfoaluminate cement: setting time and the hydration properties, Constr. Build. Mater. 51 (2014) 47–54, https://doi.org/10.1016/j.conbuildmat.2013.10.028.
[8] R.I. Iacobescu, Y. Pontikes, D. Koumpouri, G.N. Angelopoulos, Synthesis, characterization and properties of calcium ferroaluminate belite cements produced with electric arc furnace steel slag as raw material, Cem. Concr. Compos. 44 (2013) 1–8, https://doi.org/10.1016/j.cemconcomp.2013.08.002.
[9] A. Rungchet, P. Chindaprasirt, S. Wansom, K. Pimraksa, Hydrothermal synthesis of calcium sulfoaluminate–belite cement from industrial waste materials, J. Clean. Prod. 115 (2016) 273–283, https://doi.org/10.1016/j.jclepro.2015.12.068.
[10] S. Rubert, C. Angulski da Luz, M.V. F. Varela, J.I. Pereira Filho, R.D. Hooton, Hydration mechanisms of supersulfated cement, J. Therm. Anal. Calorim. 134 (2018) 971–980, https://doi.org/10.1007/s10973-018-7243-6.
[11] S. Choi, J.-M. Kim, D. Han, J.-H. Kim, Hydration properties of ladle furnace slag powder rapidly cooled by air, Constr. Build. Mater. 113 (2016) 682–690, https://doi.org/10.1016/j.conbuildmat.2016.03.089.
[12] L. Pelletier, F. Winnefeld, B. Lothenbach, The ternary system Portland cement–calcium sulphoaluminate clinker–anhydrite: hydration mechanism and mortar properties, Cem. Concr. Compos. 32 (2010) 497–507, https://doi.org/10.1016/j.cemconcomp.2010.03.010.
[13] L.E. Burris, K.E. Kurtis, Influence of set retarding admixtures on calcium sulfoaluminate cement hydration and property development, Cem. Concr. Res. 104 (2018) 105–113, https://doi.org/10.1016/j.cemconres.2017.11.005.
[14] M. Lanzón, P.A. García-Ruiz, Effect of citric acid on setting inhibition and mechanical properties of gypsum building plasters, Constr. Build. Mater. 28 (2012) 506–511, https://doi.org/10.1016/j.conbuildmat.2011.06.072.
[15] G. Camarini, M.C.C. Pinto, A.G. de Moura, N.R. Manzo, Effect of citric acid on properties of recycled gypsum plaster to building components, Constr. Build. Mater. 124 (2016) 383–390, https://doi.org/10.1016/j.conbuildmat.2016.07.112.
[16] A.M. Cody, H. Lee, R.D. Cody, P.G. Spry, The effects of chemical environment on the nucleation, growth, and stability of ettringite [Ca3Al(OH)6]2(SO4)3·26H2O, Cem. Concr. Res. 34 (2004) 869–881, https://doi.org/10.1016/j.cemconres.2003.10.023.
[17] E. Adesanya, K. Ohenoja, P. Kinnunen, M. Illikainen, Alkali activation of ladle slag from steel-making process, J. Sustain. Metall. (2016) 1–11, https://doi.org/10.1007/s40831-016-0089-x.
[18] H. Nguyen, P. Kinnunen, V. Carvelli, M. Mastali, M. Illikainen, Strain hardening polypropylene fiber reinforced composite from hydrated ladle slag and gypsum, Compos. Part B Eng. 158 (2019) 328–338, https://doi.org/10.1016/j.compositesb.2018.09.056.
[19] European Standard, EN 196-1, Methods of Testing Cement - Part 1: Determination of Strength, European Committee for Standardization, 1040 Brussels, Belgium, 2016.
[20] European Standard, EN 196-2, Methods of Testing Cement - Part 2: Chemical Analysis of Cement, European Committee for Standardization, 1040 Brussels, Belgium (2013).
[21] ASTM International, ASTM C494, Standard Specification for Chemical Admixtures for Concrete, ASTM International, West Conshohocken, PA, 2017www.astm.org.
[22] G. Möschner, B. Lothenbach, R. Figi, R. Kretzschmar, Influence of citric acid on the hydration of Portland cement, Cem. Concr. Res. 39 (2009) 275–282, https://doi.org/10.1016/j.cemconres.2009.01.005.
[23] L. Wadsö, Operational issues in isothermal calorimetry, Cem. Concr. Res. 40 (2010) 1129–1137, https://doi.org/10.1016/j.cemconres.2010.03.017.
[24] L. Lutterotti, S. Matthies, H.R. Wenk, MAUD (Material Analysis Using Diffraction): a user friendly java program for Rietveld texture analysis and more, in: Jerzy A. Szpunar (Ed.), Proc. Twelfth Int. Conf. Textures Mater. ICOTOM-12, National Research Press, Montreal, 1999, p. 1599.
[25] L. Lutterotti, MAUD: Material Analysis Using Diffraction, (n.d.). http://maud.radiographema.eu/ ((accessed January 8, 2019)).
[26] H.M. Rietveld, A profile refinement method for nuclear and magnetic structures, J. Appl. Crystallogr. 2 (1969) 65–71, https://doi.org/10.1107/S0021889869006558.
[27] C. Hesse, F. Goetz-Neunhoeffer, J. Neubauer, A new approach in quantitative in-situ XRD of cement pastes: correlation of heat flow curves with early hydration reactions, Cem. Concr. Res. 41 (2011) 123–128, https://doi.org/10.1016/j.cemconres.2010.09.014.
[28] M. Merlini, G. Artioli, T. Cerulli, F. Cella, A. Bravo, Tricalcium aluminate hydration in additivated systems. A crystallographic study by SR-XRPD, Cem. Concr. Res. 38 (2008) 477–486, https://doi.org/10.1016/j.cemconres.2007.11.011.
[29] J. Skibsted, E. Henderson, H.J. Jakobsen, Characterization of calcium aluminate phases in cements by aluminum-27 MAS NMR spectroscopy, Inorg. Chem. 32 (1993) 1013–1027, https://doi.org/10.1021/ic00058a043.
[30] J. Rottstegge, M. Wilhelm, H.W. Spiess, Solid state NMR investigations on the role of organic admixtures on the hydration of cement pastes, Cem. Concr. Compos. 28 (2006) 417–426, https://doi.org/10.1016/j.cemconcomp.2005.12.002.
[31] N.B. Singh, A.K. Singh, S. Prabha Singh, Effect of citric acid on the hydration of portland cement, Cem. Concr. Res. 16 (1986) 911–920, https://doi.org/10.1016/0008-8846(86)90015-3.
[32] D. Jansen, F. Goetz-Neunhoeffer, B. Lothenbach, J. Neubauer, The early hydration of Ordinary Portland Cement (OPC): an approach comparing measured heat flow with calculated heat flow from QXRD, Cem. Concr. Res. 42 (2012) 134–138, https://doi.org/10.1016/j.cemconres.2011.09.001.
[33] V.S. Ramachandran, M.S. Lowery, Conduction calorimetric investigation of the effect of retarders on the hydration of Portland cement, Thermochim. Acta 195 (1992) 373–387, https://doi.org/10.1016/0040-6031(92)80081-7.
[34] D. Jansen, F. Goetz-Neunhoeffer, C. Stabler, J. Neubauer, A remastered external standard method applied to the quantification of early OPC hydration, Cem. Concr. Res. 41 (2011) 602–608, https://doi.org/10.1016/j.cemconres.2011.03.004.
[35] J. Cheung, A. Jeknavorian, L. Roberts, D. Silva, Impact of admixtures on the hydration kinetics of Portland cement, Conf. Spec. Cem. Hydration Kinet. Model. Quebec City 2009 CONMOD10 Lausanne 2010, 41 2011, pp. 1289–1309, , https://doi.org/10.1016/j.cemconres.2011.03.005.
[36] P. Bentz Dale, A. Peltz Max, W. John, Early-age properties of cement-based materials. II: influence of water-to-cement ratio, J. Mater. Civ. Eng. 21 (2009) 512–517, https://doi.org/10.1061/(ASCE)0899-1561(2009)21:9(512).
[37] Y. Jeong, C.W. Hargis, S.-C. Chun, J. Moon, The effect of water and gypsum content on strätlingite formation in calcium sulfoaluminate-belite cement pastes, Constr. Build. Mater. 166 (2018) 712–722, https://doi.org/10.1016/j.conbuildmat.2018.01.153.
[38] D. Jansen, A. Spies, J. Neubauer, D. Ectors, F. Goetz-Neunhoeffer, Studies on the early hydration of two modifications of ye'elimite with gypsum, Cem. Concr. Res. 91 (2017) 106–116, https://doi.org/10.1016/j.cemconres.2016.11.009.
[39] C.W. Hargis, A.P. Kirchheim, P.J.M. Monteiro, E.M. Gartner, Early age hydration of calcium sulfoaluminate (synthetic ye'elimite, C4A3S¯) in the presence of gypsum and varying amounts of calcium hydroxide, Cem. Concr. Res. 48 (2013) 105–115, https://doi.org/10.1016/j.cemconres.2013.03.001.
[40] F. Winnefeld, B. Lothenbach, Hydration of calcium sulfoaluminate cements — experimental findings and thermodynamic modelling, Cem. Concr. Res. 40 (2010) 1239–1247, https://doi.org/10.1016/j.cemconres.2009.08.014.
[41] S.W. Tang, H.G. Zhu, Z.J. Li, E. Chen, H.Y. Shao, Hydration stage identification and phase transformation of calcium sulfoaluminate cement at early age, Constr. Build. Mater. 75 (2015) 11–18, https://doi.org/10.1016/j.conbuildmat.2014.11.006.
[42] F. Winnefeld, L.H.J. Martin, C.J. Müller, B. Lothenbach, Using gypsum to control hydration kinetics of CSA cements, Constr. Build. Mater. 155 (2017) 154–163, https://doi.org/10.1016/j.conbuildmat.2017.07.217.
[43] Y. Liao, X. Wei, G. Li, Early hydration of calcium sulfoaluminate cement through electrical resistivity measurement and microstructure investigations, Constr. Build. Mater. 25 (2011) 1572–1579, https://doi.org/10.1016/j.conbuildmat.2010.09.042.
[44] G. Paul, E. Boccaleri, L. Buzzi, F. Canonico, D. Gastaldi, Friedel's salt formation in sulfoaluminate cements: a combined XRD and 27Al MAS NMR study, Cem. Concr. Res. 67 (2015) 93–102, https://doi.org/10.1016/j.cemconres.2014.08.004.
[45] A. Gruskovnjak, B. Lothenbach, F. Winnefeld, R. Figi, S.-C. Ko, M. Adler, U. Mäder, Hydration mechanisms of super sulphated slag cement, Cem. Concr. Res. 38 (2008) 983–992, https://doi.org/10.1016/j.cemconres.2008.03.004.
[46] D. Gastaldi, G. Paul, L. Marchese, S. Irico, E. Boccaleri, S. Mutke, L. Buzzi, F. Canonico, Hydration products in sulfoaluminate cements: evaluation of amorphous phases by XRD/solid-state NMR, Cem. Concr. Res. 90 (2016) 162–173, https://doi.org/10.1016/j.cemconres.2016.05.014.
[47] J. Zhang, X. Guan, H. Li, X. Liu, Performance and hydration study of ultra-fine sulfoaluminate cement-based double liquid grouting material, Constr. Build. Mater. 132 (2017) 262–270, https://doi.org/10.1016/j.conbuildmat.2016.11.135.
[48] C. Hu, D. Hou, Z. Li, Micro-mechanical properties of calcium sulfoaluminate cement and the correlation with microstructures, Cem. Concr. Compos. 80 (2017) 10–16, https://doi.org/10.1016/j.cemconcomp.2017.02.005.
[49] ASTM International, ASTM C1600, Standard Specification for Rapid Hardening Hydraulic Cement, ASTM International, West Conshohocken, PA, 2017www.astm.org.